The theoretical prediction of infrared spectra of *trans*- and *cis*-hydroxycarbene calculated using full dimensional *ab initio* potential energy and dipole moment surfaces

Lucas Koziol,[1] Yimin Wang,[2] Bastiaan J. Braams,[2] Joel M. Bowman,[2] and Anna I. Krylov[1,a)]
[1]*Department of Chemistry, University of Southern California, Los Angeles, California 90089-0482, USA*
[2]*C.L. Emerson Center for Scientific Computation, Department of Chemistry, Emory University, Atlanta, Georgia 30322, USA*

(Received 22 February 2008; accepted 18 April 2008; published online 29 May 2008)

Accurate infrared spectra of the two hydroxycarbene isomers are computed by diagonalizing the Watson Hamiltonian including up to four mode couplings using full dimensional potential energy and dipole moment surfaces calculated at the CCSD(T)/cc-pVTZ (frozen core) and CCSD/6-311G** (all electrons correlated) levels, respectively. Anharmonic corrections are found to be very important for these elusive higher-energy isomers of formaldehyde. Both the energy levels and intensities of stretching fundamentals and all overtone transitions are strongly affected by anharmonic couplings between the modes. The results for *trans*-HCOH/HCOD are in excellent agreement with the recently reported IR spectra, which validates our predictions for the *cis*-isomers. © *2008 American Institute of Physics*. [DOI: 10.1063/1.2925452]

I. INTRODUCTION

Hydroxycarbene, HCOH, is a high energy (2.2 eV) diradicaloid isomer of formaldehyde, separated by a barrier of about 3.7 eV.[1–8] It is believed to play a role in the photochemistry of formaldehyde and in the interstellar media.[1–3] Recently, possible role of hydroxycarbene in the reaction of carbon atom with water has been considered.[7,8]

Due to its relatively mild diradical character (the ground state is a singlet, and the ST gap is about 1 eV), this is a well behaved system from the electronic structure point of view, and it has been computationally characterized.[2–5,7,8] The $H_2CO \rightarrow HCOH$ isomerization was discussed in classical and quantum molecular dynamics simulations of the lowest dissociation channel, $H_2CO \rightarrow H_2+CO$.[9–11] These isomers are also contained in the *ab initio* global potential energy surface of Zhang *et al.*[12] and they play a role in the interesting "roaming" dynamics in the H_2CO photodissociation.[13]

It was suggested that HCOH can be derived from formaldehyde following protonation of the oxygen.[5,6] Hydroxycarbene has been produced in the photodissociation of CH_2OH and CH_2OD, albeit with some internal energy,[14] which enabled the determination of its heat of formation. When the internal energy exceeds the dissociation barrier, it has been shown to decompose either directly/or via isomerization to formaldehyde.[14] As we learned during the final stages of the manuscript preparation, Schreiner *et al.* have successfully synthesized *trans*-HCOH and HCOD and recordered their IR spectra in argon matrix.[15] They reported that HCOH is relatively short lived even in cryogenic environment and rearranges to formaldehyde with the half-life of about 2 h. The deuterated species, HCOD, however, has been found to be very stable at these conditions. The assignment of the observed IR band origins was supported by variational calculations of vibrational energy levels using CCSD(T)/cc-pCVQZ quartic force field.[15] The differences between the computed and experimental values were less than 1% for all the observed transitions except for the two fundamental transitions, ν_1 in HCOH and ν_2 in HCOD, for which the deviations were 1.7% and 1.4%, respectively.

The lowest energy isomer, *trans*-hydroxycarbene, is 0.20 eV below the *cis*-isomer, and is separated by a relatively low barrier of 0.96 eV, as shown in Fig. 1. The observed fast rearrangement of HCOH to formaldehyde via tunneling through a higher barrier of 1.50 eV suggests even shorter lifetimes of *cis*-HCOH, which, however, might be increased by deuteration.

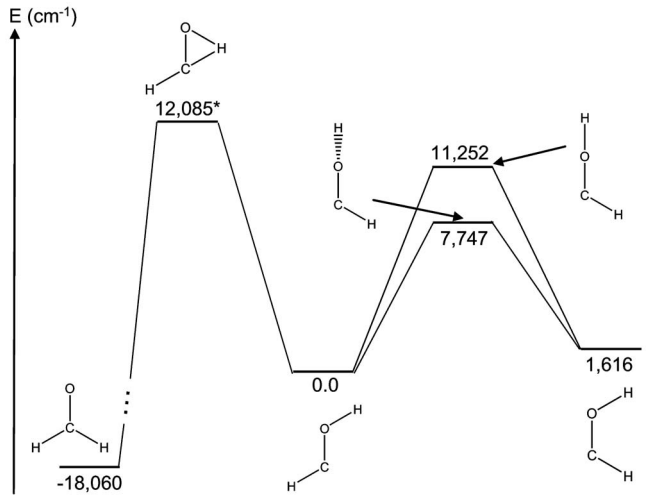

FIG. 1. Stationary points on the HCOH PES. The subspace connecting formaldehyde with *trans*-hydroxycarbene (marked with *) is not defined on our surface fits: At this point, CCSD(T)/cc-pVTZ energy at B3LYP/cc-pVTZ optimized transition state is shown for reference.

a)Electronic mail: krylov@usc.edu.

TABLE I. Comparison of harmonic frequencies (cm^{-1}) and IR intensities (km/mol, in parentheses) for *trans*-hydroxycarbene.

	Mode	Symmetry	cc-pVTZ[a]	cc-pVTZ[b]	PES[c]	aug-cc-pVTZ[b]	cc-pVQZ[b]
ν_6	o.p. wag	a''	1101 (117)	1091	1098	1086	1093
ν_5	i.p. bend	a'	1218 (139)	1215	1214	1209	1218
ν_4	CO stretch	a'	1339 (64)	1327	1326	1312	1318
ν_3	i.p. bend	a'	1520 (19)	1514	1508	1506	1513
ν_2	CH stretch	a'	2882 (139)	2855	2853	2863	2863
ν_1	OH stretch	a'	3773 (81)	3754	3754	3740	3754

[a]ACES II using analytic gradients, all electrons are correlated.
[b]MOLPRO using total energies, core electrons are frozen.
[c]Finite-difference calculations using PES fitted to the cc-PVTZ (frozen core) results.

To be of a benchmark value for experimentalists, anharmonic corrections should be taken into account even for the fundamental transitions in rigid molecules, e.g., in formaldehyde they are of 3%–5% of the harmonic frequencies.[16,17] Their magnitude increases for overtone transitions. For the higher-energy isomers, *cis*- and *trans*-HCOH, the potential energy surface (PES) exhibits stronger anharmonicities, and the harmonic IR spectrum is quite different from the exact one. Lower symmetry of HCOH can also contribute to larger anharmonicities.

We report computed IR spectra of the two hydroxycarbene isomers. We combine high-level *ab initio* calculations of potential energy and dipole moment surfaces (DMS) with numerically accurate calculations of vibrational levels and wave functions. The latter are used to evaluate IR intensities. Excellent agreement between the experimental spectra and our results for the *trans*-isomer suggests that the predicted spectra for *cis*-HCOH/HCOD are accurate as well, and can aid in a future experimental characterization of the *cis*-isomer. Moreover, our full dimenional PES covering both isomers and the transition barriers between them can be used to investigate isomerization dynamics.

II. THEORY AND COMPUTATIONAL DETAILS

The vibrational levels and wave functions of HCOH were calculated by diagonalizing the full Watson Hamiltonian[18] for $J=0$ (pure vibration) in the basis constructed using vibrational self-consistent field (VSCF) functions. The VSCF calculations employed harmonic oscillator wave functions along the normal coordinates as the one-dimensional basis set for the optimized VSCF modals. Basis functions with quantum numbers from 0 to 15 were included for each modal, with corresponding harmonic frequency. These were contracted to six numerical functions. Multimode interactions in the PES were included up to the four-mode level and rovibrational (Watson correction and Coriolis) interactions up to three-mode level. The basis for virtual state vibrational configuration interaction (VCI) calculations consisted of all VSCF product wave functions with maximum of five-tuple excitations from the reference in each mode, with maximum of four modes excited, with the added restriction of a maximum sum of quanta of 10. The matrix elements of the Hamiltonian were numerically calculated by potential optimized quadrature with ten integration points.

This procedure was employed to calculate vibrational energies and intensities that were used to compute the IR spectra presented below. Most of the CI energies are converged to within 1 cm^{-1}. Only for seven of the states above 3000 cm^{-1} for the *cis*-HCOH and *cis*-HCOD isomers, the convergence is about 2–3 cm^{-1}.

For benchmark purposes, we also conducted vibrational Rayleigh–Schrödinger perturbation theory calculations for *trans*-HCOH. We employed second-order Møller-Plesset scheme (VMP2) as described in Refs. 19 and 20. These calculations included three-mode couplings in the potential and neglected rovibration terms. They are compared to VSCF and VCI results obtained at the same level of theory. All these calculations employed ten basis functions in each mode. These VCI/VMP2 calculations included up to eight-tuple excitations.

Vibrational calculations employed a full dimensional PES. The PES covers the *trans*- and *cis*-isomers and the two

TABLE II. Comparison of harmonic frequencies (cm^{-1}) and IR intensities (km/mol, in parentheses) for *cis*-hydroxycarbene.

	Mode	Symmetry	cc-pVTZ[a]	cc-pVTZ[b]	PES[c]	aug-cc-pVTZ[b]	cc-pVQZ[b]
ν_6	o.p. wag	a''	1028 (27)	1016	1014	1011	1020
ν_5	i.p. bend	a'	1238 (44)	1235	1238	1228	1235
ν_4	CO stretch	a'	1345 (69)	1331	1335	1315	1331
ν_3	i.p. bend	a'	1491 (42)	1483	1476	1471	1479
ν_2	CH stretch	a'	2794 (195)	2764	2768	2772	2797
ν_1	OH stretch	a'	3662 (17)	3650	3655	3628	3651

[a]ACES II using analytic gradients, all electrons are correlated.
[b]MOLPRO using total energies, core electrons are frozen.
[c]Finite-difference calculations using PES fitted to the cc-pVTZ (frozen core) results.

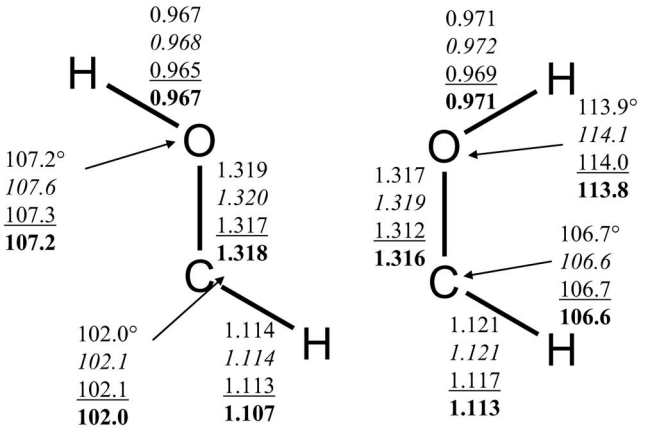

FIG. 2. CCSD(T)/cc-pVTZ (regular print), CCSD(T)/aug-cc-pVTZ (italics), CCSD(T)/cc-pVQZ (underlined), and PES (bold) equilibrium structures of *trans*-(left) and *cis*-(right) hydroxycarbene. $E_{\mathrm{nuc}}=30.631\,859$ a.u. and $E_{\mathrm{nuc}}=30.557\,941$ a.u. for *trans*- and *cis*-isomers, respectively, at the CCSD(T)/cc-pVTZ (frozen core) equilibrium structure.

barriers connecting them, see Fig. 1. It is an eigth degree polynomial in the set of internuclear bond lengths, represented in a specially constructed basis invariant to permutations of like nuclei. The polynomial has 1613 terms, which are fitted by least squares to 17 262 *ab initio* single points, calculated by the CCSD(T) method[21,22] with the cc-pVTZ basis set.[23] There are 12 949 points in the energy range $[0,0.1]$ hartrees above the lower minimum (the *trans*-equilibrium structure) 2341 points in the range $[0.1,0.2]$ hartrees and 1542 points above 0.2 hartrees (these latter points are mostly fragment data and highly twisted configurations to enforce asymptotes). The rms fitting errors in these energy regions are 43, 123, and 134 cm^{-1} respectively. The PES reproduces harmonic frequencies at the two minima within 7 cm^{-1} of the *ab initio* values (see Tables I and II) and correctly describes asymptotic behavior of the CO, CH, and OH stretches. Numerical frequencies on the PES are calculated by fivefold central finite differences with

TABLE III. HCOH VCI energy levels (cm^{-1}) and IR intensities (km/mol).

		trans-		*cis*-	
No.	state label	Energy	Intensity	Energy	Intensity
1	ν_6	1060	119.66	978	34.90
2	ν_5	1177	131.74	1189	47.00
3	ν_4	1295	75.53	1299	76.00
4	ν_3	1475	22.32	1442	41.55
5	$2\nu_6$	2097	1.01	1942	1.30
6	$\nu_5+\nu_6$	2240	0.10	2166	0.45
7	$2\nu_5$	2347	2.37	2368	3.43
8	$\nu_4+\nu_6$	2352	0.03	2268	0.03
9	$\nu_4+\nu_5$	2461	1.96	2471	2.10
10	$\nu_3+\nu_6$	2521	0.33	2421	0.74
11	$2\nu_4$	2569	0.76	2579	0.04
12	$\nu_3+\nu_5$	2622	23.25	2650	69.19
13	ν_2	2691	116.08	2552	161.07
14	$\nu_3+\nu_4$	2776	24.00	2736	1.42
15	$2\nu_3$	2952	1.92	2885	7.88
16	$3\nu_6$	3113	0.00	2895	0.05
17	$\nu_5+2\nu_6$	3280	0.00	3124	0.17
18	$\nu_4+2\nu_6$	3384	0.01	3221	0.00
19	$2\nu_5+\nu_6$	3416	0.00	3333	0.04
20	$3\nu_5$	3510	0.34	3545	0.44
21	$\nu_4+\nu_5+\nu_6$	3525	0.02	3441	0.02
22	ν_1	3553	51.59	3397	10.90
23	$\nu_3+2\nu_6$	3545	2.65	3385	0.07
24	$2\nu_4+\nu_6$	3622	0.00	3536	0.01
25	$\nu_4+2\nu_5$	3620	0.00	3631	0.13
26	$\nu_3+\nu_5+\nu_6$	3676	0.08	3622	0.57
27	$2\nu_4+\nu_5$	3724	0.00	3730	0.05
28	$\nu_2+\nu_6$	3743	0.35	3519	2.13
29	$\nu_3+2\nu_5$	3770	0.01	3830	0.47
30	$3\nu_4$	3824	0.00	3841	0.01
31	$\nu_3+\nu_4+\nu_6$	3825	0.08	3712	0.01
32	$\nu_2+\nu_5$	3853	0.71	3713	1.69
33	$\nu_3+\nu_4+\nu_5$	3923	0.11	3935	0.10
34	$\nu_2+\nu_4$	3973	0.35	3849	0.35
35	$2\nu_3+\nu_6$	3984	0.00	3861	0.02
36	$\nu_2+\nu_3$	⋯	⋯	3952	0.33
37	$4\nu_6$	⋯	⋯	3943	0.02

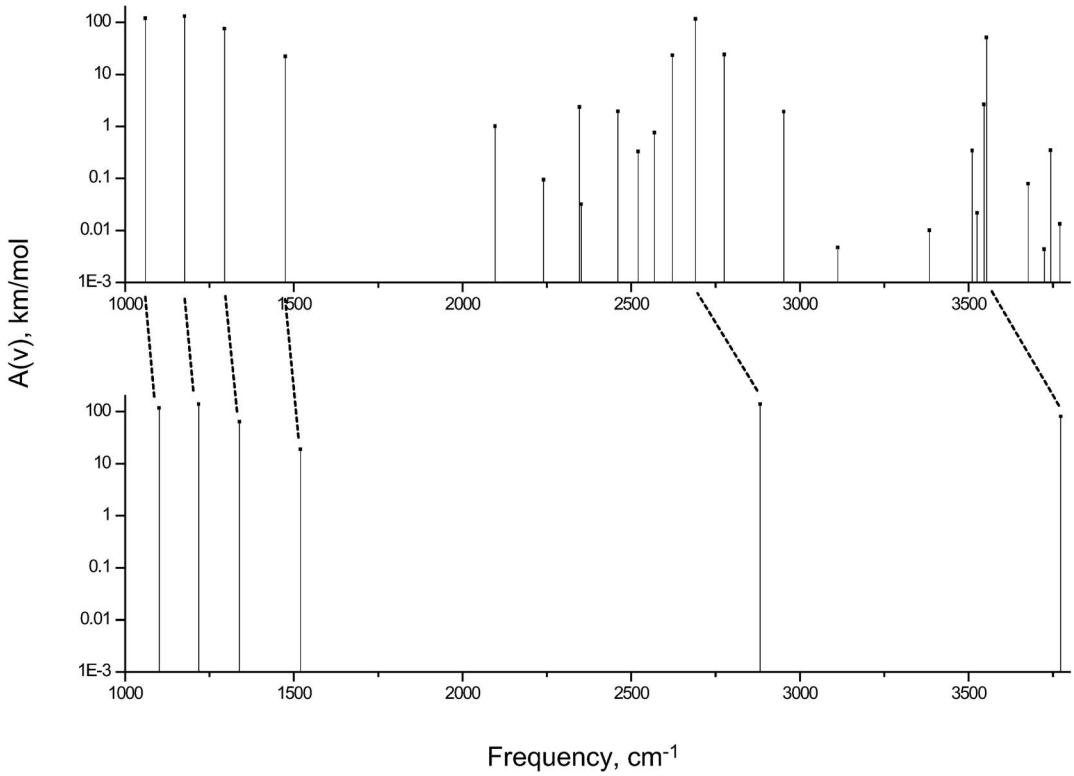

FIG. 3. VCI (top) and harmonic (bottom) IR spectrum for *trans*-HCOH.

step size of 0.01 Å. Similarly constructed PESs have been used in several dynamics and spectroscopy studies and details of constructing the symmetrized polynomial basis are given elsewhere.[24] The DMS was fitted to the same set of geometries as the PES, at the CCSD/6-311G** level of theory.

Basis set effects were investigated by calculating equilibrium geometries and harmonic frequencies with the aug-cc-pVTZ and cc-pVQZ bases[23] (see Tables I and II and Fig. 2 for comparison). In both isomers, changes in equilibrium angles are less than 0.1°. In the *trans*-isomer, bond lengths are converged to 0.002 Å. In the *cis*-isomer, bond lengths slightly decrease with increasing basis set size. The largest change is in the CO bond, with 0.005 Å difference between the cc-pVTZ and cc-pVQZ bases. For the *trans*-isomer, changes in harmonic frequencies are less than 10 cm^{-1} between the cc-pVTZ and cc-pVQZ bases, and slightly larger between cc-pVTZ and aug-cc-pVTZ. For the *cis*-isomer, the differences are within 4 cm^{-1} for all the modes except the CH stretch that changes by 32 cm^{-1} between cc-pVTZ and cc-pVQZ. This mode is also very sensitive to core electron treatment.

Single point energies and dipole moments for the fitting were calculated using MOLPRO (Ref. 25) and Q-CHEM (Ref. 26), respectively. Harmonic frequencies and IR intensities were calculated using MOLPRO and ACES II,[27] respectively. The core orbitals were frozen in all MOLPRO calculations, and correlated in ACES II and Q-CHEM calculations. MOLPRO harmonic vibrational frequencies were computed by finite differences using total energies, whereas ACES II calculations employed first analytic derivatives.[28] CCSD dipole moments were computed using analytic gradients and properties code.[29]

The MULTIMODE program was used for all vibrational energy and intensity calculations.[30] Additional VSCF, VCI, and VMP2 calculations were performed using new code developed at USC.

III. RESULTS AND DISCUSSION

A. The IR spectrum of HCOH

Harmonic frequencies and intensities for the HCOH isomers are given in Tables I and II. Multimode VCI excitation energies below 4000 cm^{-1} and corresponding anharmonic intensities are given in Table III. Intensities are reported within a threshold of 0.01 km/mol. The two sets are also depicted as stick spectra in Figs. 3 and 4. VMP2 results are presented in Table IV, which also contains VCI and VSCF results obtained at the same level of theory (see Sec. II for the details).

The four lowest transitions lying below 1600 cm^{-1} are 0-1 transitions for out-of-plane wag, two in-plane bends, and the CO stretch. Anharmonic corrections for the frequencies and intensities of these modes are small and result in slightly lower frequencies. VMP2 and VCI are within 5 cm^{-1} from each other. In the 1600–3000 cm^{-1} region, there is only one harmonic frequency, the ν_2 CH stretch. However, when anharmonicities are taken into account, the spectra become more complex. In the *trans*-isomer, ν_2 has intensity of 116.1 km/mol, and two combination bands also have non-negligible intensity: $\nu_3+\nu_5$ and $\nu_3+\nu_4$, at 23.3 and 24.0 km/mol, respectively. VMP2 behavior becomes more erratic, especially for higher overtones, e.g., the VMP2-VCI

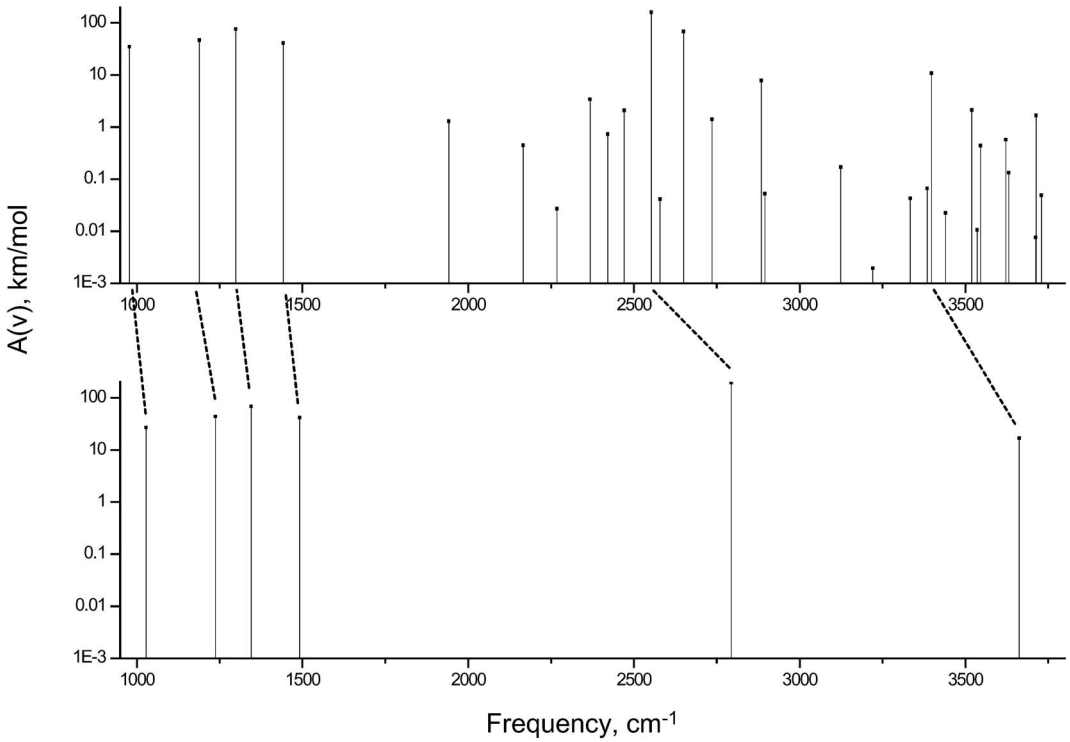

FIG. 4. VCI (top) and harmonic (bottom) IR spectrum for *cis*-HCOH.

differences of 60–75 cm^{-1} were observed for two overtones in this energy range.

For the seven experimental IR bands reported, multimode VCI calculations closely match the experiment. Differences are typically less than 12 cm^{-1} (less than 1%), with the exception of the OH stretch, ν_1, where the VCI frequency is 52 cm^{-1} higher than the experimental value. This frequency was similarly overestimated in the CCSD(T)/cc-pCVQZ quartic force field calculations.[15] The close agreement between the two sets of theoretical data suggests that the discrepancies between the theoretical and experimental values are largely due to the matrix-induced shifts.

Intensities of the transitions calculated using multimode VCI wave functions are also in excellent agreement with the experiment, i.e., the computed values are within 2%–7% of experiment except for the ν_2 stretch, for which the observed

TABLE IV. VSCF, VCI and VMP2 results (using USC code, see text) for *trans*-HCOH.

No.	State label	VSCF	VMP2	VCI	VMP2-VCI
1	ν_6	1054	1042	1042	0
2	ν_5	1187	1166	1171	−5
3	ν_4	1297	1294	1293	1
4	ν_3	1483	1471	1473	−2
5	$2\nu_6$	2107	2116	2058	58
6	$\nu_5+\nu_6$	2239	2196	2208	−12
7	$2\nu_5$	2386	2383	2333	50
8	$\nu_4+\nu_6$	2346	2346	2330	16
9	$\nu_4+\nu_5$	2480	2458	2453	5
10	$\nu_3+\nu_6$	2521	2497	2499	−2
11	$2\nu_4$	2575	2570	2567	3
12	$\nu_3+\nu_5$	2682	2681	2606	75
13	ν_2	2674	2678	2688	−10
14	$\nu_3+\nu_4$	2775	2773	2773	0
15	$2\nu_3$	2968	2947	2947	0
16	$3\nu_6$	3170	3175	3056	119
17	$\nu_5+2\nu_6$	3289	3289	3221	68
18	$\nu_4+2\nu_6$	3395	3380	3342	38
19	$2\nu_5+\nu_6$	3433	3346	3370	−24
20	$3\nu_5$	3594	3532	3490	42
21	$\nu_4+\nu_5+\nu_6$	3528	3525	3485	40
22	ν_1	3507	3517	3543	−26

TABLE V. Normal coordinates, harmonic frequencies (cm^{-1}) and IR intensities (km/mol) of HCOD at the CCSD(T)/cc-pVTZ level with all electrons being correlated.

	Mode	Symmetry	*trans*-HCOD	*cis*-HCOD
ν_6	o.p. wag	a''	941 (81)	889 (0)
ν_5	i.p. bend	a'	951 (67)	952 (12)
ν_4	CO stretch	a'	1331 (104)	1333 (88)
ν_3	i.p. bend	a'	1459 (9)	1456 (32)
ν_2	OD stretch	a'	2744 (66)	2660 (29)
ν_1	CH stretch	a'	2885 (116)	2800 (172)

intensity is lower than the theoretical value by a factor of 2.4. The wave function of this state is heavily mixed and includes significant contributions from three VSCF configurations. We expect that the degree of mixing, which is crucial for determining the intensity, might be strongly affected by the matrix environment.

In the *cis*-isomer, only the $\nu_3+\nu_5$ transition has significant intensity (69.2 km/mol), compared to the *cis*-ν_2 stretch of 161.1 km/mol. Several transitions in this region also acquire intensities of 1–3 km/mol, well within experimental reach.

In the harmonic approximation, there is only one line, ν_1 (OH stretch), with nonzero intensity above 3000 cm^{-1}. In *trans*-HCOH, the VCI ν_1 fundamental transition has the highest intensity (51.6 km/mol), followed by a neighboring combination/overtone, $\nu_3+2\nu_6$ (2.7 km/mol). Transitions to all other states have intensity below 1 km/mol. In *cis*-HCOH, ν_1 has intensity of 10.9 km/mol, and two states acquire 1–2 km/mol intensity.

The anharmonic corrections for the two hydrogen stretches are about 200–250 cm^{-1} for both isomers; their intensities are also more strongly affected than those of the four lowest modes. VMP2 very accurately reproduces this value. Most notable is the OH stretch for the *trans*-isomer, which is 81 km/mol in the double-harmonic approximation (DHA) and 52 km/mol when computed with VCI wave functions and DMS. Consistently, anharmonicities slightly lowered intensities for all fundamentals.

In the high energy region, the harmonic approximation qualitatively breaks down.

TABLE VI. HCOD VCI energy levels (cm^{-1}) and IR intensities (km/mol).

		trans-		*cis*-	
No.	state label	Energy	Intensity	Energy	Intensity
1	ν_6	908	78.80	847	1.54
2	ν_5	925	60.61	921	11.77
3	ν_4	1287	119.56	1288	102.37
4	ν_3	1419	10.75	1414	32.37
5	$2\nu_6$	1796	0.13	1682	0.70
6	$\nu_5+\nu_6$	1831	0.06	1767	0.22
7	$2\nu_5$	1842	0.62	1826	2.30
8	$\nu_4+\nu_6$	2190	0.06	2126	0.02
9	$\nu_4+\nu_5$	2205	0.02	2202	0.09
10	$\nu_3+\nu_6$	2321	0.28	2261	0.68
11	$\nu_3+\nu_5$	2339	0.31	2326	2.91
12	$2\nu_4$	2552	0.60	2552	0.39
13	ν_2	2622	94.38	2516	54.29
14	ν_1	2669	51.54	2584	136.20
15	$3\ \nu_6$	2667	0.00	2505	0.01
16	$\nu_3+\nu_4$	2713	30.82	2704	12.53
17	$\nu_5+2\nu_6$	2710	7.01	2598	20.12
18	$2\nu_5+\nu_6$	2749	0.00	2665	0.00
19	$3\nu_5$	2754	0.03	2720	0.21
20	$2\nu_3$	2851	16.15	2834	14.20
21	$\nu_4+2\nu_6$	3072	0.03	2953	0.02
22	$\nu_4+\nu_5+\nu_6$	3108	0.00	3043	0.00
23	$\nu_4+2\nu_5$	3116	0.00	3099	0.08
24	$\nu_3+2\nu_6$	3204	0.03	3094	0.05
25	$\nu_3+\nu_5+\nu_6$	3242	0.00	3173	0.08
26	$\nu_3+2\nu_5$	3251	0.00	3230	0.02
27	$2\nu_4+\nu_6$	3450	0.02	3382	0.01
28	$2\nu_4+\nu_5$	3463	0.00	3461	0.00
29	$\nu_2+\nu_6$	3526	0.05	3358	1.23
30	$\nu_2+\nu_5$	3536	0.94	3428	2.53
31	$\nu_1+\nu_6$	3573	0.76	3421	0.85
32	$\nu_1+\nu_5$	3584	0.13	3500	0.29
33	$4\nu_6$	3578	0.00	3379	0.01

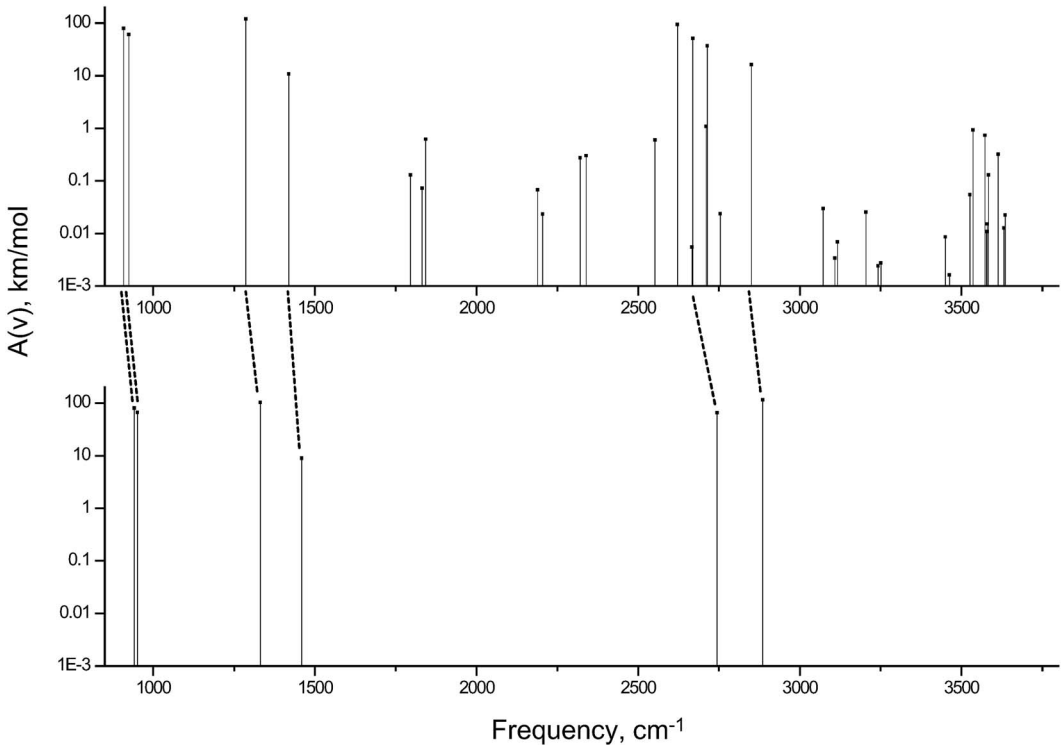

FIG. 5. VCI (top) and harmonic (bottom) IR spectrum for *trans*-HCOD.

B. Deuterated hydroxycarbene: HCOD

Harmonic frequencies and intensities for the HCOD isomers are given in Table V . Lower vibrational frequencies cause a higher density of states; thus, VCI states up to 3600 cm^{-1} are reported (Table VI). The spectra are visualized in Figs. 5 and 6.

Harmonic frequencies for HCOD are smaller than HCOH due to the higher nuclear mass of deuterium. Within the adiabatic approximation, potential energy and dipole surfaces (including equilibrium structures) are the same for the two species; only the normal coordinate vectors differ, as the nuclear masses affect the Hessian. Intensities are indirectly related to mass through the normal coordinates and their derivatives.

Behavior of the lowest four modes is similar to HCOH. However, the energy region of the stretches (2500–3000 cm^{-1}) exhibits different patterns. Anharmonicities bring the two stretches closer in frequency. Also, for both isomers, they lower the intensity of ν_2 and increase that of ν_1, which reverses the relative ratio of intensities in *trans*-HCOD, i.e., the ratios of the intensities of the ν_2 and ν_1 fundamental transitions are 0.2 and 1.8 at the DHA and VCI levels, respectively. The latter value agrees well with the experimental ratio of 2.9.

Combination bands also play a larger role in the stretch region, possibly due to an increased density of states facilitating the couplings between the modes. In *trans*-HCOD, the transitions to the $\nu_3+\nu_4$ and $2\nu_3$ states acquire intensities of 30.8 and 16.2 km/mol, respectively, compared to 94.4 and 51.5 km/mol for ν_2 and ν_1 states. Both these wave functions have large (0.2-0.5) contributions from the ν_1 VSCF state. In *cis*-HCOD, the spectrum is more harmonic relative to the *trans*-isomer, similar to HCOH. The same combination bands as for *trans*-HCOD have the only non-negligible intensities, although their magnitude (12.5 and 14.2 km/mol) are smaller than for the ν_2 and ν_1 fundamentals (54.3 and 136.2 km/mol, respectively).

Eight experimental IR bands for *trans*-HCOD were reported;[15] our multimode VCI calculations show similar agreement with frequencies and intensities as for HCOH. The largest difference is a 34 cm^{-1} higher calculated frequency for ν_2 (OD stretch). Similar result was obtained in the CCSD(T)/cc-pCVQZ quartic force field calculations.[15]

IV. CONCLUSIONS

We report accurate configuration interaction calculations of vibrational levels of the *cis*- and *trans*-isomers of HCOH and HCOD. The IR spectra in the region below 4000 cm^{-1} are strongly affected by anharmonicities. Strong effects were observed for IR intensities, as anharmonic mode couplings mix the bright and dark states. For *trans*-HCOH/HCOD, frequencies and intensities are in excellent agreement with the recently reported IR spectra.[15] This agreement validates accuracy of our PES and gives predictive power to the calculated spectra of the *cis*-isomers, as well as isomerization barriers.

For the lowest four fundamentals, the DHA rather accurately reproduces both frequencies and intensities. However, for combinations and overtones, and even stretch fundamentals, inclusion of anharmonicity is necessary. Combination/overtone bands acquired intensity even in the low energy (<2500 cm^{-1}) region, which could complicate assignment of fundamental bands.

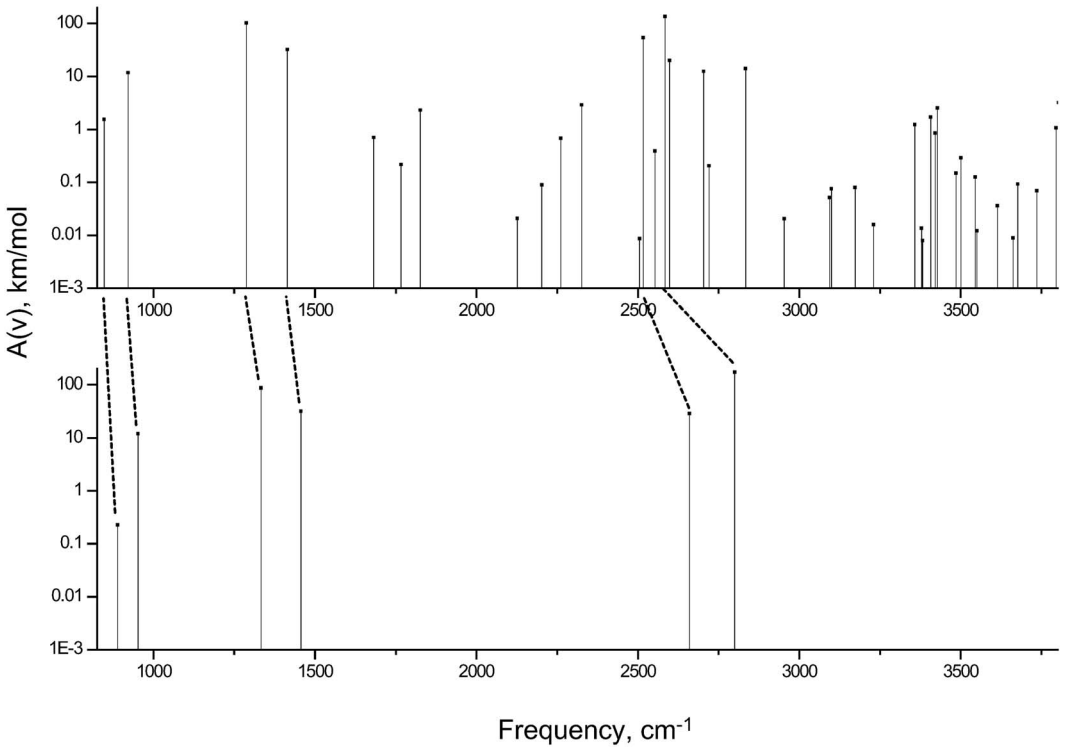

FIG. 6. VCI (top) and harmonic (bottom) IR spectrum for *cis*-HCOD.

For fundamental transitions, VMP2 very accurately reproduces the VCI results (less than 10 cm^{-1} differences for $\nu_2-\nu_6$, and 24 cm^{-1} for ν_1); however, the errors as large as 60–70 cm^{-1} were observed for some overtones, and one high-overtone state ($3\nu_6$) was overestimated by 120 cm^{-1}.

Overall, HCOH isomers exhibit higher anharmonicities than formaldehyde, a more rigid molecule of higher symmetry. For the fundamental transitions, average anharmonicity in frequencies is 3.0% in formaldehyde,[16,17] whereas in *trans*- and *cis*-HCOH it is 3.7% and 4.6%, respectively. The overtones deviate more from the harmonic values for the HCOH isomers also; the average differences between the $\nu=2$ overtones and twice the $\nu=1$ values are 8 cm^{-1} for formaldehyde, 13 cm^{-1} for *trans*-HCOH, and 10 cm^{-1} for *cis*-HCOH.

In HCOD, the higher nuclear mass led to a denser spectrum, where the effects of multimode contributions to the PES, as well as state mixing, significantly increased.

Anharmonicities generally lowered the frequencies relative to the harmonic approximation, and they very differently affected different modes, so that the spacing between vibrational levels changed. This leads to Fermi resonances not described by the DHA. Finally, the effects of anharmonicities on the intensities were found to be important. Relative to the DHA, anharmonicities tend to lower the intensity of strong peaks and increase the intensity of weak peaks owing to the state mixing.

ACKNOWLEDGMENTS

This work is conducted under the auspices of the *iOpen-Shell* Center for Computational Studies of Electronic Structure and Spectroscopy of Open-Shell and Electronically Excited Species supported by the National Science Foundation through the CRIF:CRF CHE-0625419+0624602+0625237 grant. A.I.K. and J.M.B. also acknowledge support of the Department of Energy (DE-FG02-05ER15685 and DE-FG02-97ER14782, respectively). We would like thank Professor Wesley D. Allen and co-workers for sharing with us their results prior to publication.

[1] P. L. Houston and C. B. Moore, J. Chem. Phys. **65**, 757 (1976).
[2] M. R. Hoffmann and H. F. Schaeffer III, Astrophys. J. **249**, 563 (1981).
[3] M. J. H. Kemper, J. M. F. van Dijk, and H. M. Buck, J. Am. Chem. Soc. **100**, 7841 (1978).
[4] J. G. Goddard and H. F. Schaefer, J. Chem. Phys. **70**, 5117 (1979).
[5] Y. Osamura, J. G. Goddard, and H. F. Schaefer, J. Chem. Phys. **74**, 617 (1980).
[6] S. S. Prasad and W. T. Huntress, Astrophys. J. **239**, 151 (1980).
[7] D. Hwang, A. M. Mebel, and B. Wang, Chem. Phys. **244**, 143 (1999).
[8] P. R. Schreiner and H. P. Reisenauer, ChemPhysChem **7**, 880 (2006).
[9] T. Yonehara and S. Kato, J. Chem. Phys. **125**, 084307 (2006).
[10] T. Yonehara and S. Kato, J. Chem. Phys. **117**, 11131 (2002).
[11] G. F. Bauerfeldt, L. M. M. de Albuquerque, G. Arbilla, and E. C. da Silva, J. Mol. Spectrosc. **580**, 147 (2002).
[12] X.-B. Zhang, S.-L. Zou, L. B. Harding, and J. M. Bowman, J. Phys. Chem. A **108**, 8980 (2004).
[13] D. Townsend, S. A. Lahankar, S. K. Lee, S. D. Chambreau, A. G. Suits, X. Zhang, J. Rheinecker, L. B. Harding, and J. M. Bowman, Science **306**, 1158 (2004).
[14] L. Feng and H. Reisler, J. Phys. Chem. A **108**, 9847 (2004); L. Feng, A. V. Demyanenko, and H. Reisler, J. Chem. Phys. **120**, 6524 (2004).
[15] P. R. Schreiner, H. P. Reisenauer, F. Pickard, A. C. Simmonett, W. D. Allen, E. Mátyus, and A. G. Császár, "Capture of elusive hydroxymethylene and its fast disappearance through tunneling" Nature (London) (in press).
[16] P. Seidler, J. Kongsted, and O. Christiansen, J. Phys. Chem. A **111**, 11205 (2007).
[17] G. Rauhut, J. Chem. Phys. **121**, 9313 (2004).
[18] J. K. G. Watson, Mol. Phys. **15**, 479 (1968).
[19] L. Norris, M. Ratner, E. Roitberg, and R. Gerber, J. Chem. Phys. **105**, 11261 (1996).

[20] O. Christiansen, J. Chem. Phys. **119**, 5773 (2003).
[21] K. Raghavachari, G. W. Trucks, J. A. Pople, and M. Head-Gordon, Chem. Phys. Lett. **157**, 479 (1989).
[22] J. D. Watts, J. Gauss, and R. J. Bartlett, J. Chem. Phys. **98**, 8718 (1993).
[23] T. H. Dunning, J. Chem. Phys. **90**, 1007 (1989).
[24] X. Huang, B. J. Braams, and J. M. Bowman, J. Phys. Chem. **122**, 044308 (2005).
[25] H.-J. Werner, P. J. Knowles, R. Lindh, M. Schütz and others, MOLPRO 2002.6, 2003.
[26] Y. Shao, L. F. Molnar, Y. Jung, J. Kussmann, C. Ochsenfeld, S. Brown, A. T. B. Gilbert, L. V. Slipchenko, S. V. Levchenko, D. P. O'Neil, R. A. Distasio, Jr., R. C. Lochan, T. Wang, G. J. O. Beran, N. A. Besley, J. M. Herbert, C. Y. Lin, T. Van Voorhis, S. H. Chien, A. Sodt, R. P. Steele, V. A. Rassolov, P. Maslen, P. P. Korambath, R. D. Adamson, B. Austin, J. Baker, E. F. C. Bird, H. Daschel, R. J. Doerksen, A. Drew, B. D. Dunietz, A. D. Dutoi, T. R. Furlani, S. R. Gwaltney, A. Heyden, S. Hirata, C.-P. Hsu, G. S. Kedziora, R. Z. Khalliulin, P. Klunziger, A. M. Lee, W. Z. Liang, I. Lotan, N. Nair, B. Peters, E. I. Proynov, P. A. Pieniazek, Y. M. Rhee, J. Ritchie, E. Rosta, C. D. Sherrill, A. C. Simmonett, J. E. Subotnik, H. L. Woodcock III, W. Zhang, A. T. Bell, A. K. Chakraborty, D. M. Chipman, F. J. Keil, A. Warshel, W. J. Herhe, H. F. Schaefer III, J. Kong, A. I. Krylov, P. M. W. Gill, and M. Head-Gordon, Phys. Chem. Chem. Phys. **8**, 3172 (2006).
[27] J. F. Stanton, J. Gauss, J. D. Watts, W. J. Lauderdale, and R. J. Bartlett, ACES II, 1993. The package also contains modified versions of the MOLECULE Gaussian integral program of J. Almlöf and P. R. Taylor, the ABACUS integral derivative program written by T. U. Helgaker, H. J. Aa. Jensen, P. Jørgensen, and P. R. Taylor, and the PROPS property evaluation integral code of P. R. Taylor.
[28] J. Gauss, J. F. Stanton, and R. J. Bartlett, J. Chem. Phys. **95**, 2623 (1991).
[29] S. V. Levchenko, T. Wang, and A. I. Krylov, J. Chem. Phys. **122**, 224106 (2005).
[30] J. M. Bowman, S. Carter, and X. Huang, Int. Rev. Phys. Chem. **22**, 533 (2003).